INTERNATIONAL JOURNAL OF
RADIATION ONCOLOGY • BIOLOGY • PHYSICS

www.redjournal.org

BIOLOGY CONTRIBUTION

Differential Radiobiological Effects of Alpha and Beta-Minus-Emitter Targeted Radionuclide Therapy: DNA Damage and Survival

Ruth C. Winter, PhD,[a,b] Ulrike Bauder-Wüst,[a] Martin Schäfer, Dipl-Ing (FH),[c] Yvonne Remde,[c] Mareike Roscher, PhD,[c] Ramon Lopez Perez, PhD,[d] and Martina Benešová-Schäfer, PhD[a]

[a]Junior Research Group Translational Radiotheranostics, German Cancer Research Center (DKFZ), Heidelberg, Germany; [b]Faculty of Physics and Astronomy, Heidelberg University, Heidelberg, Germany; [c]Service Unit Radiopharmaceuticals and Preclinical Studies, German Cancer Research Center (DKFZ), Heidelberg, Germany; and [d]Clinical Cooperation Unit Molecular and Radiation Oncology, German Cancer Research Center (DKFZ), Heidelberg, Germany

Received Jan 15, 2026; Revised Aug 13, 2026; Accepted for publication Aug 13, 2026

Purpose: Metastatic cancer remains a major challenge, demanding more effective and biologically informed therapeutic strategies. Targeted radionuclide therapy (TRT) holds significant promise, but limited understanding of treatment response and resistance hinders its optimization. This work aimed to improve TRT efficacy and overcome radioresistance by determining how radionuclide properties, administered activity, and subcellular localization govern radiobiological outcomes. The objectives were to advance TRT for prostate cancer, overcome radioresistance, and generate mechanistic insights to guide radiopharmaceutical design and radionuclide selection.

Methods and Materials: Prostate-specific membrane antigen (PSMA)-positive (LNCaP [lymph node adenocarcinoma of the prostate] and C4-2) and PSMA-negative (PC-3) prostate cancer cell lines were exposed to ^{225}Ac- or ^{177}Lu-labeled PSMA radiopharmaceuticals or nontargeted radionuclides for 1 or 4 hours across activity ranges for α-emitters (1-100 kBq) and β^--emitters (100-5000 kBq), with external beam radiation therapy (0.5-2.5 Gy) as a reference. DNA double-strand breaks (DSBs) were quantified by immunofluorescence-based γH2AX analysis and complemented by cell viability assays. A proof-of-concept combination study with the DNA-dependent protein kinase (DNA-PK) inhibitor Nedisertib (M3814; Selleck Chemicals, Houston, TX, USA) was performed.

Results: The α-emitters outperformed the β^--emitters, inducing comparable DSBs at only 1% of the applied activity. PSMA-mediated internalization strongly enhanced short-range α-TRT but had negligible impact on longer-range β^--TRT.

Corresponding author: Martina Benešová-Schäfer, PhD; E-mail: m.benesova@dkfz-heidelberg.de

Author Responsible for Statistical Analysis: Ruth C. Winter was responsible for the statistical analyses.

Disclosures: Various patent applications for PSMA ligands have been filed by the German Cancer Research Center DKFZ. U.B.-W., M.S., Y.R., M.R., and M.B.-S. are coinventors of this patent. The remaining authors declare that this work was conducted in the absence of any commercial or financial relationships that could be construed as a potential conflict of interest. R.C.W. was funded by the Helmholtz International Graduate School for Cancer Research (HIGS) (grant number 104515). An early stage of the project was co-funded through a collaboration with Bayer AG, Berlin, Germany, until 2023.

Data Sharing Statement: Research data are stored in an institutional repository and will be shared upon request to the corresponding author.

Acknowledgments—The authors gratefully acknowledge Prof Svetlana Selivanova and her team at Canadian Nuclear Laboratories (Chalk River, Canada) for providing ^{225}Ac and insightful scientific discussions. We also thank Dr Sabine Zitzmann-Kolbe (Bayer AG, Berlin, Germany) for supplying ^{225}Ac, ^{223}Ra (Xofigo), and ^{227}Th, and for access to laboratory facilities. We are grateful to Ina Kurth and the DKFZ Joint RadOncBio Lab for granting access to the MultiRad 225 X-ray (Faxitron) system and the Nikon Eclipse Ti2-E microscope, and we sincerely thank Rosemarie Euler-Lange for her valuable technical support.

https://www.sciencedirect.com/science/article/pii/S0360301626042276#sec0008

Supplementary material associated with this article can be found in the online version at doi:10.1016/j.ijrobp.2026.08.036.

Int J Radiation Oncol Biol Phys, Vol. 126, No. 5, pp. 1721−1732, 2026
0360-3016/$ - see front matter © 2026 The Author(s). Published by Elsevier Inc. This is an open access article under the CC BY license (http://creativecommons.org/licenses/by/4.0/)
https://doi.org/10.1016/j.ijrobp.2026.08.036

α-Induced DSBs persisted for up to 72 hours, whereas DSBs decreased over time after β^--TRT and external beam radiation therapy. Combination therapy with Nedisertib significantly enhanced TRT efficacy in C4-2 cells, enabling a 64-fold (^{225}Ac) versus 4-fold (^{177}Lu) reduction in required activity. In the least radiosensitive PC-3 cells, viability decreased to below 50% following combined α-TRT and Nedisertib treatment.

Conclusions: Our study defines key determinants for optimizing TRT. Cellular internalization is critical for short-range α-emitters, whereas β^--emitters depend on high binding affinity and retention, providing experimental guidance for radiopharmaceutical design and radionuclide selection. Distinct DNA repair kinetics underscore radionuclide-specific biological effects. Combining TRT with DNA-PK inhibition is a promising strategy to enhance efficacy, enable activity de-escalation, and potentially mitigate toxicity. © 2026 The Author(s). Published by Elsevier Inc. This is an open access article under the CC BY license (http://creativecommons.org/licenses/by/4.0/)

Introduction

An effective cancer therapy should fulfill 3 key criteria: (1) high specificity to selectively target malignant cells while sparing healthy tissue; (2) strong efficacy to eradicate tumor cells, including in advanced or metastatic disease; and (3) low toxicity to minimize adverse effects and preserve patient quality of life. Achieving this balance remains a major challenge in oncology and has driven the development of increasingly precise treatment strategies.

Targeted radionuclide therapy (TRT) represents a major step toward these goals by delivering ionizing radiation systemically and selectively to cancer cells via molecular targeting vectors. This enables selective irradiation of disseminated and metastatic disease while limiting damage to healthy tissue.[1] The recent regulatory approval of TRT agents by the U.S. Food and Drug Administration (FDA) and European Medicines Agency (EMA), like [^{177}Lu]Lu-PSMA-617 (Pluvicto; Novartis Pharmaceuticals Corporation, Basel, Switzerland) for metastatic castration-resistant prostate cancer (PCa) in 2022, has highlighted the clinical potential of TRT and expanded treatment options beyond conventional therapies.[2] Nevertheless, clinical responses remain heterogeneous, with 30% to 40% of patients either failing initial response or developing resistance over the treatment course.[3] Nonresponders are frequently characterized by alterations in DNA damage response and repair pathways, emphasizing the need for mechanistically informed strategies to improve efficacy and overcome resistance.[4,5]

Despite its growing clinical relevance, progress in TRT optimization is limited by an incomplete understanding of its underlying radiobiology. While radiobiological knowledge has been generated from a wide range of experimental systems, radiobiological models are strongly influenced by experience from external beam radiation therapy (EBRT), where radiation is delivered over short periods in fractionated schedules. In contrast, TRT delivers radiation continuously over extended periods, resulting in distinct patterns of dose rate, energy deposition, DNA damage induction, and repair.[6] These distinctions challenge the direct application of EBRT-derived radiobiological principles to TRT and demand a reassessment of the relationship between absorbed dose and biological effect. While accurate dosimetry provides the quantitative foundation for TRT, a TRT-specific radiobiological framework is needed to predict biological effects and inform treatment planning and therapy optimization.

The biological effectiveness of TRT depends on a complex interplay of multiple parameters, including physical radionuclide properties (emitter type, energy spectrum, and half-life), activity concentration and exposure time, biodistribution and tumor uptake, and cellular localization.[7] In particular, α- and β^--emitting radionuclides differ substantially in linear energy transfer, track structure, and cytotoxic potential, which may translate into distinct DNA damage signatures and repair kinetics.[8,9] Target-specific internalization mechanisms, such as prostate-specific membrane antigen (PSMA)-mediated uptake, may further enhance biological effectiveness by bringing radionuclides closer to the nucleus, particularly for short-range α-emitters. In this context, in vivo α-particle nanogenerators such as ^{225}Ac, which undergo multiple sequential α-decays, are especially attractive because of their high therapeutic potential. However, the recoil energy generated during α-decay can dissociate radioactive daughter nuclides from the targeting vector, leading to redistribution in the body and increased off-target toxicity. For example, an in vivo study demonstrated that ^{221}Fr, the first daughter nuclide of ^{225}Ac, exhibits high tissue selectivity for the salivary glands, which may contribute to the development of xerostomia observed following ^{225}Ac-based TRT.[10] Consequently, the biological fate and dosimetric impact of in vivo α-particle nanogenerators remain important areas for further investigation.

The overarching objective of this work was to provide mechanistic insights to support TRT optimization and the rational development of combination strategies to overcome intrinsic and acquired resistance. Within a controlled experimental framework, we demonstrate that radiation quality, activity, and cellular localization critically shape the extent and persistence of TRT-induced DNA damage, with α- and β^--emitters producing fundamentally distinct damage profiles. We further show that PSMA-mediated internalization enhances biological effectiveness differently across emitter types and that DNA damage induction and repair follow markedly different temporal patterns depending on radiation type. Importantly, we identify DNA-dependent protein kinase (DNA-PK) inhibition as a promising strategy to

potentiate TRT efficacy and enable activity de-escalation. Together, these findings provide a mechanistic foundation for refining TRT design and advancing combination approaches in PCa and beyond.

Methods and Materials

Detailed methods and the key resources table are provided in Table E1.

Cell culture

PCa cell lines were purchased from American Type Culture Collection (ATCC). PSMA-positive LNCaP (lymph node adenocarcinoma of the prostate, CRL-1740) and C4-2 (CRL-3314) cells and PSMA-negative PC-3 cells (CRL-1435) were cultured in RPMI 1640 Medium (PAN-Biotech, P04-16500; supplemented with 10% fetal bovine serum and 1% L-glutamine) at 37 °C and 5% CO_2. LNCaP and C4-2 cells were selected as PSMA-positive models and PC-3 cells as a PSMA-negative control, based on their established PSMA-specific uptake and internalization characteristics reported in the literature and our previous studies.[11-13]

Radionuclides and radiolabeling

The radionuclide ^{177}Lu was purchased as $^{177}LuCl_3$ from ITM Pharma Solutions in 0.04 M HCl. The radionuclide ^{225}Ac was supplied as $^{225}AcCl_3$ by Svetlana Selivanova from the Canadian Nuclear Laboratories in solid form. Additionally, ^{225}Ac was provided as $^{225}Ac(NO_3)_3$ by the European Commission−Joint Research Centre, BWXT, and Global Morpho Pharma, all as dry films. For experiments, the full-activity batch was diluted in ultrapure, metal-free 0.04 M HNO_3 (TraceMetal Grade nitric acid, 67%-69%, Fischer Scientific). The compound PSMA-617 was synthesized as reported[11,12] and used for ^{177}Lu labeling. For ^{225}Ac labeling, PSMA-716, a Macropa-based variant, was derived directly from the clinically established PSMA-617 scaffold through a chelator swap, while retaining the PSMA-targeting pharmacophore and linker architecture. PSMA-716 was employed due to the favorable radiochemical properties of the Macropa chelator for actinium complexation, including efficient labeling under mild conditions, high radiochemical yields, and excellent complex stability. The synthesis of PSMA-716 is described in Figure E1.

Radiolabeling was performed directly before the individual treatments. For ^{177}Lu labeling, 50 μL of sodium acetate (0.4 M, pH 5.0), 5 to 10 μL of $^{177}LuCl_3$ (20 MBq), and 1 μL of 1 mM PSMA-617 (1 nmol) were mixed and incubated for 30 minutes at 95 °C. The specific activity was approximately 20 MBq/nmol. For ^{225}Ac labeling, 50 μL of tris(hydroxymethyl)aminomethane (TRIS; 0.1 M, pH 7.0), 5 to 10 μL of $^{225}Ac(NO_3)_3$ (1 MBq), and 4 μL of 0.5 mM PSMA-716 (2 nmol) were mixed and incubated for 15 minutes at 95 °C. The specific activity was approximately 0.5 MBq/nmol. Radiochemical purity (RCP) was assessed by radio-reversed-phase thin-layer chromatography (radio-RP-TLC) prior to use (RCP > 95%; see Supplementary Material Appendix E1).

DNA damage assay via γH2AX immunofluorescent staining

Cells grown on transwell inserts (0.4 μm pore size; preventing migration) were exposed for 4 hours to PSMA-bound or nontargeted ($^{177}LuCl_3$ and $^{225}AcCl_3$) radioactivity in 300 μL per insert. Applied total activities per insert were 1, 5, 10, and 100 kBq for ^{225}Ac, or 100, 500, 1000, and 5000 kBq for ^{177}Lu. For a 1-hour exposure, total activities were 5 and 10 kBq for ^{225}Ac, or 500 and 1000 kBq for ^{177}Lu. External photon irradiation was delivered using the MultiRad225 X-ray irradiation system (Faxitron Bioptics, LLC, USA) at doses of 0.5 to 2.5 Gy (see Supplementary Material Appendix E1). All time points are reported relative to the start of treatment. Thus, for the standard 4-hour radionuclide incubation protocol, the 4-hour time point corresponds to the end of radionuclide exposure, whereas the 24-, 48-, and 72-hour time points include additional post-treatment incubation periods in fresh medium. For external photon irradiation, which lasted less than 2 minutes, time points were likewise referenced to the start of treatment. At the indicated time points, cells were fixed with paraformaldehyde, permeabilized with 0.5% Triton X-100 (Sigma-Aldrich) in Dulbecco's phosphate-buffered saline (DPBS), and stained with Image-iT FX signal enhancer (Thermo Fisher Scientific), γH2AX antibody (Biozol Diagnostica), Alexa Fluor 488-labeled secondary antibody (Thermo Fisher Scientific), and 4′,6-diamidin-2-phenylindol (Thermo Fisher Scientific, DAPI). Excised insert membranes were mounted in Fluoromount-G (Biozol Diagnostica) and imaged using a Nikon Eclipse Ti2-E inverted microscope. γH2AX foci were quantified using MATLAB-based (MathWorks) image analysis (refer to Fig. E2).

Cell viability assessed by resazurin assay in mono and combination therapy

Cells were seeded 24 hours prior to treatment (day 0) in 96-well flat-bottom plates at densities of 1750 (LNCaP), 1300 (C4-2), and 1000 (PC-3) cells per well. Each experimental condition was performed in quadruplicate. Treatment with the DNA-PK inhibitor Nedisertib (M3814; Selleck Chemicals) was administered at concentrations of 0.01, 0.1, 1, 5, 10, and 50 μM for 24 hours prior to radionuclide exposure (150 μL/well). Afterward, cells were exposed to either PSMA-bound or nontargeted radionuclides for 4 hours at activity concentrations of 78, 313, 1250, and 5000 kBq/mL for ^{177}Lu, or 0.156, 0.625, 2.5, and 10 kBq/mL for ^{225}Ac (150 μL/well). Following treatment, cells were incubated at 37 °C until day 8. Inhibitor-only control groups

were included at all concentrations and evaluated in the absence of irradiation. Cell viability was assessed by incubating cells in resazurin-supplemented medium (10%; 165 μL/well) for 2.5 hours, followed by fluorescence measurement using a Varioskan LUX plate reader (Thermo Fisher Scientific; excitation: 530 nm and emission: 590 nm).

Statistical analyses

Statistical analyses were performed in Jupyter Notebook (version 6.5.7, Python 3.12.7) using the statsmodels package. Means and SDs were calculated from raw data from independent biological replicates. Differences between treatment conditions were assessed using a 2-way analysis of variance (ordinary least squares model) with treatment and activity as factors, including their interaction; control samples were excluded. Comparisons were made between PSMA-bound and nontargeted radionuclides, and between combination therapy (TRT + Nedisertib) and TRT monotherapy. For statistical annotation and interpretation, only the main effect of treatment was considered, representing activity-independent differences across the tested activity range. Statistical significance is indicated using standard notation ($^{*}P < .05$, $^{**}P < .01$, $^{***}P < .001$, n.s., not significant).

Results

To investigate the radiobiological effects of targeted α- and β^{-}-emitting radionuclides, we systematically analyzed DNA damage and cellular responses in PSMA-positive (C4-2 and LNCaP) and PSMA-negative (PC-3) PCa cell lines. Cells were exposed to PSMA-bound or nontargeted ^{225}Ac or ^{177}Lu across defined activity ranges and exposure times, and external photon irradiation was additionally applied as a reference. DNA damage and repair were assessed via γH2AX immunofluorescence at multiple time points, complemented by long-term cell viability assays to evaluate treatment response. In addition, combination therapy was investigated by assessing the effects of DNA-PK inhibition with Nedisertib across different concentrations on cell viability. Results for C4-2 and PC-3 cell lines are presented here, while LNCaP data are provided in Figures E3-E7.

α-Emitters require 100-fold lower activity than β^{-}-emitters to induce comparable DNA damage

To quantitatively compare DNA damage induced by α- and β^{-}-emitting radionuclides, γH2AX analysis was conducted across a range of activity levels (4-hour exposure), with external photon irradiation as the radiobiological reference (fixed at 0.5 hours postirradiation). DNA damage was quantified per nucleus based on the number of γH2AX foci, area, and mean total γH2AX intensity.

Across both PCa cell lines, α-induced foci were consistently larger and brighter than those induced by β^{-}-particles or external irradiation (Fig. 1). Compared with untreated controls (ratio = 1), ^{225}Ac increased foci area (C4-2: 1.11; PC-3: 1.05), whereas ^{177}Lu and external irradiation produced smaller foci (^{177}Lu: 0.94 vs 0.96; photons: 0.79 vs 0.78). Mean foci intensity followed a similar trend, with the largest increase relative to control observed for ^{225}Ac (C4-2: 1.72; PC-3: 1.38), with smaller increases for ^{177}Lu (1.30 vs 1.22) and photons (1.40 vs 1.22), which showed comparable effects.

Across activity levels, α-particles generated comparable numbers of γH2AX foci at 100-fold lower activity than β^{-}-particles. Mean foci count per nucleus was 4.5 to 8.6 for ^{225}Ac, 4.0 to 10.8 for ^{177}Lu, and 8.3 to 13.4 for photons (minimum-maximum values; Table 1). For ^{225}Ac, the foci count plateaued at 10 kBq, while the total γH2AX signal continued to increase up to 100 kBq, indicating underestimation of foci numbers due to signal overlap from dense α-tracks (Figs. 1 and 2).

In contrast, ^{177}Lu showed a continuous, activity-dependent increase in foci number up to 5000 kBq. Because both ^{177}Lu and photons produced smaller, well-separated foci, overlap was minimal, and total γH2AX intensity closely matched the detected foci counts.

PSMA-mediated internalization enhances DNA damage for α-emitters but not for β^{-}-emitters

To assess the contribution of internalized versus membrane-bound activity, γH2AX assays were performed using both PSMA-bound radionuclides and nontargeted ^{225}Ac or ^{177}Lu. The PSMA-negative PC-3 cell line, which does not internalize the ligand, served as a control.

In PSMA-positive C4-2, internalized ^{225}Ac induced significantly higher foci than nontargeted activity, whereas no significant difference was observed in the PSMA-negative PC-3 control (Fig. 2 and Fig. E3). In contrast, internalization did not increase DNA damage from ^{177}Lu in either cell line; in fact, nontargeted activity produced slightly higher γH2AX levels. On average, PSMA-bound ^{225}Ac increased DNA damage by a factor of 1.3 relative to nontargeted activity, whereas ^{177}Lu showed a ratio of 0.9, indicating no benefit from internalization.

These findings were further supported by cell viability assays. In C4-2 cells, ^{225}Ac reduced cell viability more strongly when PSMA-bound, whereas ^{177}Lu showed no significant difference between PSMA-bound and nontargeted activity, with nontargeted activity producing slightly stronger effects. In PC-3 cells, ^{225}Ac again showed a slight increase for nontargeted activity, while ^{177}Lu remained nonsignificant.

Delayed γH2AX increase after TRT evident in short-term repair kinetics

As shown in Figure 3A, early DNA damage induction was assessed by comparing γH2AX levels after 1 and 4 hours of

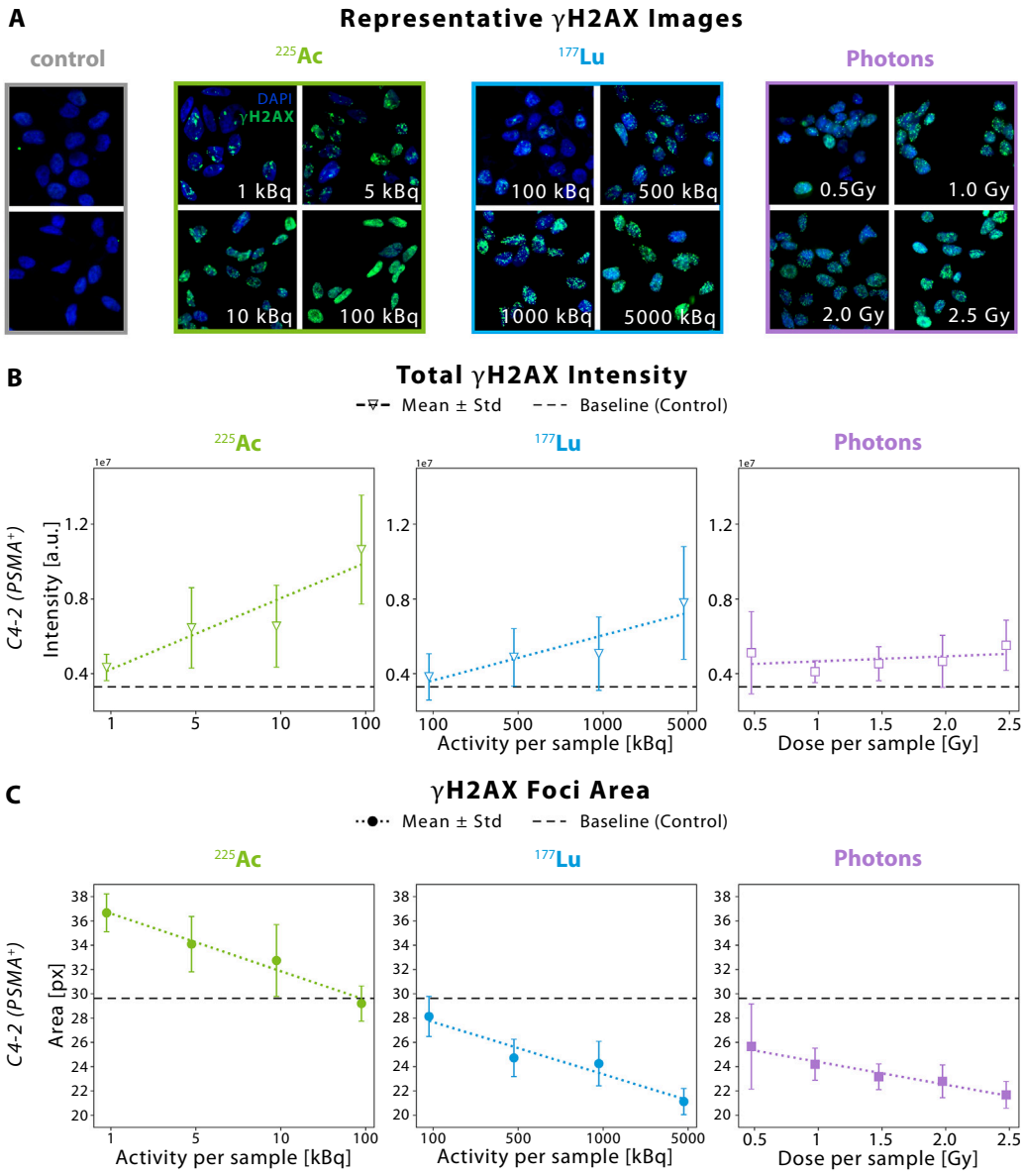


Fig. 1. Characteristics of γH2AX foci following targeted radionuclide therapy and external photon irradiation. C4-2 cells were exposed to prostate-specific membrane antigen (PSMA)-targeted ^{225}Ac- or ^{177}Lu-labeled radioligands for 4 hours at the indicated activities and then fixed, or were irradiated with external photons at the indicated absorbed doses and fixed at 0.5 hours postirradiation. γH2AX foci were assessed by immunofluorescence microscopy as a marker of DNA double-strand breaks. (A) Representative images, along with quantification of (B) total γH2AX signal intensity and (C) foci area, are shown to provide an overview of radiation-induced foci characteristics across different radiation types. Dotted lines represent linear fits across activity or dose ranges (excluding control values), while the horizontal gray dashed line indicates the baseline (untreated control). *Abbreviations:* DAPI = 4′,6-diamidin-2-phenylindol.

exposure. Following 1-hour exposure, γH2AX levels were lower immediately after treatment than at the 1-hour (+3 hours) time point, which includes an additional 3-hour recovery period. This increase, observed for both radionuclides, reflects continued DNA double-strand break (DSB) recognition and residual radionuclide activity. Notably, γH2AX levels after 4 hours of exposure exceeded those after 1 hour (+3 hours). In contrast, external photon irradiation showed lower γH2AX levels at 4 hours than at 0.5 hours, when most irradiation-induced DNA damage is recognized and marked by γH2AX phosphorylation.

Long-term γH2AX persistence after α-TRT but efficient repair after β⁻-TRT

To characterize DNA-damage repair kinetics, γH2AX levels were monitored up to 72 hours after treatment (after 4

Table 1 DNA damage induced by TRT and external photon irradiation.

Cell line	*Activity [^{225}Ac] [kBq]*	*1*	*5*	*10*	*100*			
C4-2	PSMA-bound	7.1 ± 1.5	8.7 ± 2.0	8.6 ± 2.0	6.7 ± 1.9			
	non-targeted	4.5 ± 0.8	6.7 ± 1.7	7.4 ± 1.9	5.0 ± 1.6			
PC-3	PSMA-bound	5.4 ± 2.6	6.4 ± 1.1	8.2 ± 1.3	5.3 ± 2.1			
	non-targeted	5.5 ± 0.7	7.3 ± 1.0	6.8 ± 1.4	4.9 ± 1.8			
	Activity [^{177}Lu] [kBq]	*100*	*500*	*1000*	*5000*			
C4-2	PSMA-bound	4.9 ± 1.3	7.1 ± 1.4	8.9 ± 1.5	14.1 ± 2.7			
	non-targeted	5.6 ± 1.1	9.8 ± 1.3	10.9 ± 3.9	13.7 ± 1.6			
PC-3	PSMA-bound	3.9 ± 0.8	5.7 ± 0.8	7.5 ± 0.7	10.9 ± 1.1			
	non-targeted	4.5 ± 0.8	8.2 ± 0.7	6.0 ± 2.9	11.6 ± 0.9			
	Photons [Gy]	*0.5*	*1*	*1.5*	*2*	*2.5*		
C4-2		10.0 ± 4.4	10.4 ± 1.0	11.0 ± 2.2	11.5 ± 1.3	12.9 ± 2.4		
PC-3		13.4 ± 3.5	8.3 ± 2.2	10.5 ± 2.7	9.0 ± 0.9	10.7 ± 2.1		
	Timepoints	*0.5 h*	*1 h*	*1 h (+3h)*	*4 h*	*24 h*	*48 h*	*72 h*
C4-2	control	3.3 ± 0.9	2.8 ± 0.7	2.8 ± 1.0	2.8 ± 1.0	2.2 ± 0.6	2.4 ± 0.9	2.1 ± 0.4
	^{225}Ac [5kBq] PSMA-bound		6.0 ± 1.1	7.5 ± 1.3	8.7 ± 2.0	9.2 ± 2.8	7.3 ± 0.7	9.7 ± 0.7
	^{177}Lu [500 kBq] PSMA-bound		4.1 ± 0.6	4.6 ± 1.6	7.1 ± 1.4	2.5 ± 0.3		
	Photons [2.5 Gy]	12.9 ± 2.4			11.2 ± 0.1	3.3 ± 0.3	2.6 ± 0.2	
PC-3	control	4.7 ± 0.9	2.9 ± 1.2	3.5 ± 1.0	3.5 ± 1.0	3.4 ± 1.3	4.9 ± 0.3	4.6 ± 1.6
	^{225}Ac [5 kBq] PSMA-bound		4.3 ± 1.3	4.8 ± 0.6	6.4 ± 1.1	5.9 ± 0.6	6.8 ± 1.2	6.7 ± 0.4
	^{177}Lu [500 kBq] PSMA-bound		2.9 ± 1.3	3.4 ± 1.0	5.7 ± 0.8	3.1 ± 1.7		
	Photons [2.5 Gy]	10.7 ± 2.1			9.7 ± 0.5	6.8 ± 0.1	5.7 ± 0.7	

Mean γH2AX foci numbers per nucleus ± standard deviation are shown for PSMA-targeted and non-targeted exposure to ^{225}Ac and ^{177}Lu for 4 h exposure. Corresponding data for external photon irradiation (0.5–2.5 Gy) are included for comparison. Graphical representation of these data is provided in Fig. 2. Values represent a minimum of three independent experimental repetitions.

hours of TRT exposure). Long-term analysis was performed using 2 activity levels per radionuclide: 5 and 10 kBq for ^{225}Ac and 500 and 1000 kBq for ^{177}Lu.

After external photon irradiation, the γH2AX signal declined progressively and returned near baseline by 48 hours. ^{177}Lu showed a similar pattern, approaching baseline by 24 hours. In contrast, ^{225}Ac-induced γH2AX levels remained elevated at all late time points and persisted throughout the entire 72-hour observation period. Between 24 and 72 hours, foci numbers increased by an average of 3-fold in C4-2 cells and 2-fold in PC-3 cells compared with controls (Fig. 3B and Figs. E4 and E5).

This persistent DNA damage may explain the markedly greater difference in efficacy between ^{225}Ac and ^{177}Lu observed in the 8-day cell viability assay (Fig. E6). Despite the ^{225}Ac:^{177}Lu activity ranges differing by a factor of 1:500 compared with 1:100 for the γH2AX assay, ^{177}Lu did not achieve reductions in viability comparable to those of ^{225}Ac. In PSMA-positive C4-2 cells, the lowest ^{225}Ac activity (0.156 kBq/mL) produced a viability reduction equivalent to the highest ^{177}Lu activity (5000 kBq/mL), corresponding to a 32,000-fold difference. At the highest activity concentrations, ^{225}Ac reduced viability to 20% PSMA-bound and 27% nontargeted, whereas ^{177}Lu reduced viability to 54% PSMA-bound and 29% nontargeted. In PSMA-negative PC-3 cells, ^{225}Ac caused substantial reductions (51% nontargeted and 64% PSMA-bound) only at 10 kBq/mL. In contrast, ^{177}Lu reduced viability to 91% nontargeted and 93% PSMA-bound, indicating minimal long-term impact of the β^--emitter. All values are normalized to untreated controls.

Combination with a DNA-PK inhibitor enhances TRT efficacy and enables substantial activity de-escalation

Because TRT primarily exerts its cytotoxic effects through DNA damage, the DNA-dependent protein kinase inhibitor Nedisertib was investigated as a potential radiosensitizer in combination with TRT. Given the central role of DNA-PK

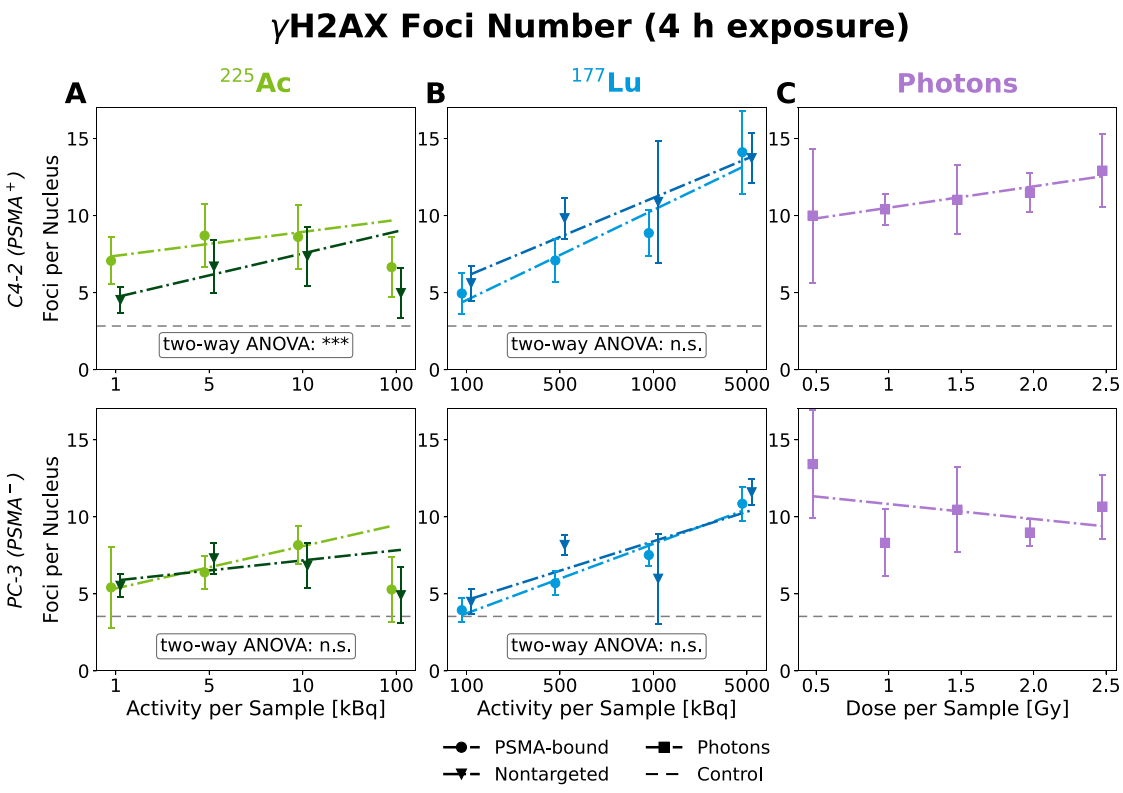


Fig. 2. DNA damage induced by different radiation types: prostate-specific membrane antigen (PSMA)-bound and nontargeted activity. Cells were exposed to either nontargeted or PSMA-bound ^{225}Ac or ^{177}Lu for 4 hours at the indicated activities, followed by immediate fixation. External photon irradiation was applied at the indicated absorbed doses, and cells were fixed at 0.5 hours postirradiation. γH2AX foci were quantified by immunofluorescence microscopy as a marker of DNA double-strand breaks and are expressed as the mean number of foci per cell. Upper row: PSMA-positive C4-2 cells exposed to increasing activities of (A) ^{225}Ac and (B) ^{177}Lu, and to increasing absorbed doses of (C) external photon irradiation. For ^{225}Ac-based targeted radionuclide therapy, correct γH2AX foci quantification at the highest activity (100 kBq) was not feasible due to extensive foci overlap (see Fig. 1). Lower row: data for PSMA-negative PC-3 cells. Dash-dotted lines represent linear fits across activity or dose ranges (excluding control values), while the horizontal gray dashed line indicates the baseline (untreated control). Statistical analysis was performed using a 2-way analysis of variance (ANOVA) to assess differences between PSMA-targeted and nontargeted conditions. $^{*}P < .05$, $^{**}P < .01$, $^{***}P < .001$, n.s., not significant.

in repairing radiation-induced DNA double-strand breaks via nonhomologous end joining, we hypothesized that DNA-PK inhibition would enhance TRT efficacy and enable comparable biological effects at lower radionuclide activities. To identify minimally cytotoxic concentrations for the combination studies, Nedisertib monotherapy (0.01-50 μM) was evaluated, which yielded half-maximal inhibitory concentration (IC_{50})values of 6.35 μM (C4-2) and 9.13 μM (PC-3). Therefore, concentrations of 0.1 and 1 μM were selected for subsequent combination experiments.

Across both radionuclides and external photon irradiation, combination treatment enhanced therapeutic efficacy relative to monotherapy, with the greatest benefit observed for α-TRT. For ^{225}Ac, the lowest combination (0.1 μM Nedisertib + 0.156 kBq/mL) produced a viability reduction equivalent to that of the highest monotherapy activity (10 kBq/mL), corresponding to a 64-fold lower activity. For ^{177}Lu, the activity reduction factor was smaller (4-fold), with comparable effects observed for 1 μM Nedisertib + 1250 kBq/mL and 5000 kBq/mL ^{177}Lu alone (Fig. 4 and Table 1; LNCaP Fig. E7).

In the least radiosensitive PC-3 cell line, only the α-TRT combination (1 μM + 10 kBq/mL) achieved a substantial viability reduction, decreasing to 34% of control levels (Table 2). The corresponding β^{-}-TRT combination (1 μM + 5000 kBq/mL) was markedly less effective (81%). As with monotherapy, the maximum reduction in this cell line was limited, reaching 51% (^{225}Ac) and 91% (^{177}Lu).

Discussion

A comprehensive understanding of radiobiology and careful dosimetry are essential for effective therapy planning, treatment refinement, and outcome prediction. While these principles are well established in EBRT, TRT introduces additional complexity due to continuous low-dose-rate

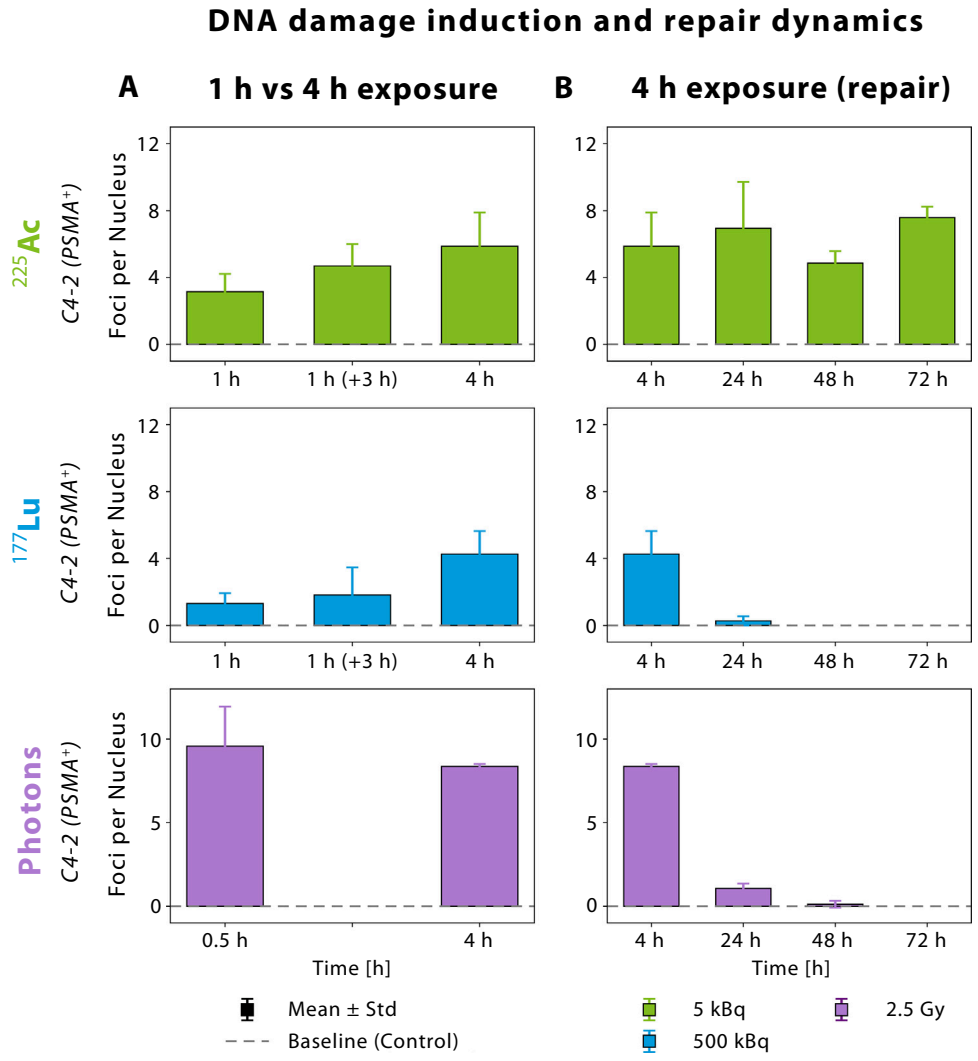


Fig. 3. Temporal dynamics of DNA damage following targeted radionuclide therapy and external photon irradiation. DNA damage was quantified by γH2AX foci at the indicated time points. Cells were exposed to prostate-specific membrane antigen (PSMA)-bound ^{225}Ac (5 kBq), ^{177}Lu (500 kBq), or external photon irradiation (2.5 Gy), as indicated. (A) Cells were exposed for either 1 or 4 hours. DNA damage was assessed either immediately after exposure or after an additional recovery period following medium replacement (eg, 1 + 3 hours indicates 1 hour exposure followed by 3 hours repair time). For photon irradiation, exposure was delivered within minutes, and DNA damage was measured at 0.5 and 4 hours postexposure. (B) At the late time point observation, cells were exposed for 4 hours, and DNA damage was monitored over extended recovery periods. Time points represent the total time from the start of exposure (4, 24, 48, and 72 hours). A decrease in γH2AX foci over time reflects DNA repair. Values represent the mean number of γH2AX foci per nucleus from independent replicates ± SD. DNA damage kinetics are shown as an example of the PSMA-positive C4-2 cell line after a single administered activity or dose. Additional activities and cell lines are presented in the Supplementary Material (Figs. E4 and E5).

exposure, heterogeneous radionuclide distribution, and emitter-specific radiobiological properties.[6] With [^{177}Lu]Lu-PSMA-617 gaining increasing relevance in clinical practice, challenges related to treatment optimization, toxicity management, and resistance mechanisms are becoming evident, underscoring the need to refine TRT strategies for PCa. Improved mechanistic insight is therefore critical to enhance efficacy while reducing treatment-related toxicities such as xerostomia.[14]

In this context, we aimed to advance the radiobiological understanding of the clinically most relevant radionuclides, ^{225}Ac and ^{177}Lu. Our study reveals fundamental radiobiological distinctions among the radionuclides in activity requirements, dependence on internalization, and DNA damage response, linking these to long-term effects on cell viability. Furthermore, we demonstrate that combining TRT with DNA-PK inhibition improves therapeutic efficacy, enables activity de-escalation, and sensitizes less responsive tumor cells.

Studies comparing the radiobiological effects of ^{225}Ac and ^{177}Lu in a unified experimental workflow are scarce, as most investigations focus on a single radionuclide due to

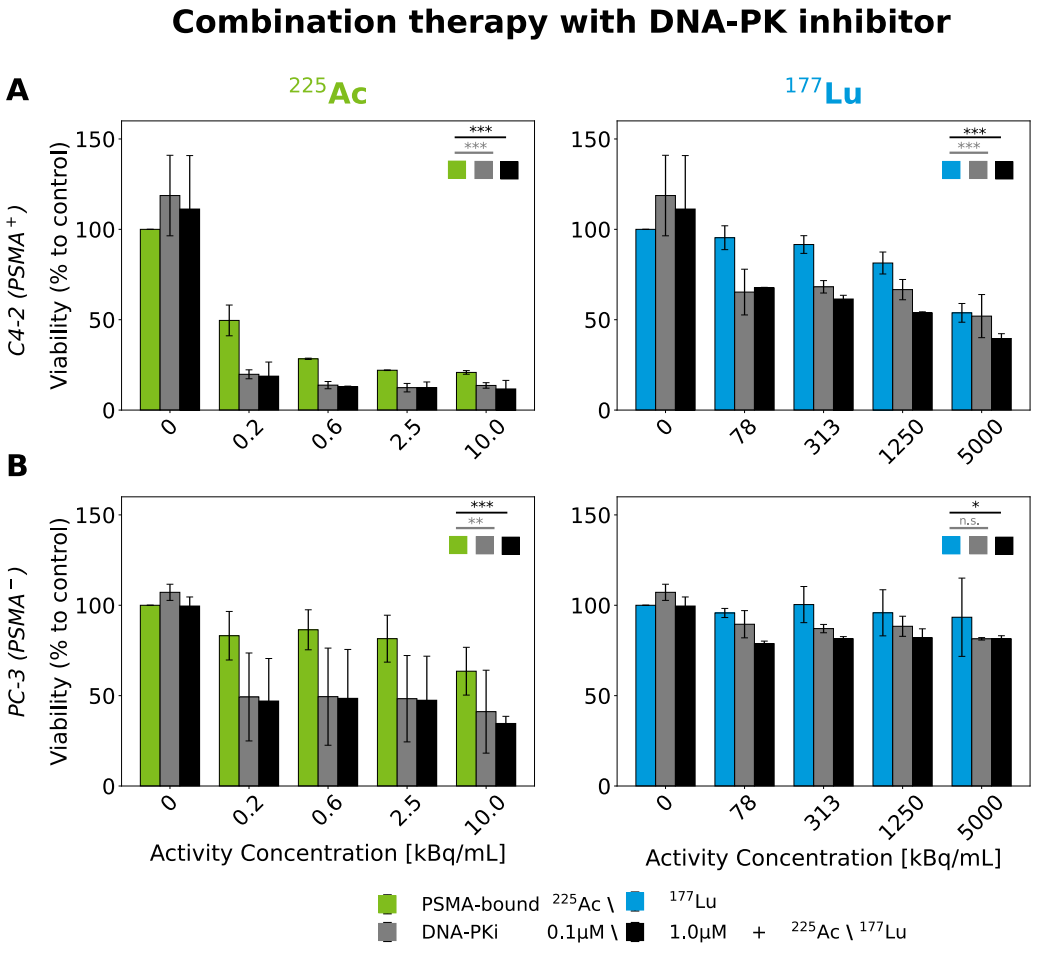


Fig. 4. Effect of DNADNA-dependent protein kinase (DNA-PK) inhibition on targeted radionuclide therapy (TRT)-induced reduction in cell viability. Cells were pretreated with the DNA-dependent protein kinase inhibitor (DNA-PKi) Nedisertib for 24 hours, followed by 4 hours of exposure to radionuclides at the indicated activities. Cell viability was assessed on day 8 using a resazurin-based fluorescence assay. Fluorescence signals were normalized to untreated controls and expressed as a percentage of the control (%). (A) Prostate-specific membrane antigen (PSMA)-positive C4-2 cells treated with PSMA-bound ^{225}Ac or ^{177}Lu. Combination treatment enhanced the reduction in cell viability more than TRT alone for both radionuclides, with effects observed at low activities for ^{225}Ac. (B) PSMA-negative PC-3 cells treated with PSMA-bound ^{225}Ac or ^{177}Lu. Combination treatment remained more effective than monotherapy, with a stronger effect observed for ^{225}Ac. For ^{177}Lu TRT, enhancement was evident only at the higher Nedisertib concentration. Bars represent mean ± SD from independent experiments. Statistical analysis was performed using a 2-way analysis of variance comparing combination treatment with the corresponding TRT monotherapy. $^{*}P < .05$, $^{**}P < .01$, $^{***}P < .001$, n.s., not significant.

limited accessibility. A standardized approach is therefore essential, as published studies vary widely in exposure times, activity ranges, assay formats, and endpoints, complicating cross-study interpretation. A few studies have compared α- and β^--emitter radioligands, including [^{225}Ac]Ac-PSMA-617 versus [^{177}Lu]Lu-PSMA-617 in PSMA-positive PCa cells and [^{225}Ac]Ac-DOTATOC versus [^{177}Lu]Lu-DOTATOC in somatostatin-receptor models.[15,16] While these studies consistently conclude that ^{225}Ac is more potent than ^{177}Lu, they did not assess internalization effects, long-term DNA damage persistence, or repair kinetics, and used heterogeneous treatment conditions compared with our investigations. Our study addresses these limitations by using a uniform workflow with defined treatment durations, multiple activity levels, long-term DNA damage and viability endpoints, and external photon irradiation as a radiobiological reference.

Although the superior effectiveness of α-particles is well established due to their high linear energy transfer and ability to induce direct complex DNA damage,[17,18] our data quantify this difference across broad activity ranges and demonstrate that α:β^- potency ratios are highly TRT parameter- and assay-dependent. For the 4-hour exposure, we observed ratios of 1:100 in γH2AX analyses and approximately 1:500 in long-term (8-day) viability assays. These findings help explain variability across studies, including reported ratios of 1:300 in antiproliferative assays[16] and 1:700 for γH2AX formation after 48 hours of treatment in

Table 2 Effect of combined TRT and DNA-PK inhibition on cellular metabolic activity.

Cell line	*Activity [^{225}Ac] [kBq]*	*0.0*	*0.2*	*0.6*	*2.5*	*10.0*
C4-2	Ac-PSMA alone	100.0 ± 0.0	49.6 ± 8.5	28.4 ± 0.4	22.0 ± 0.2	20.8 ± 1.0
	Ac-PSMA + 0.1 μM	118.7 ± 22.3	19.8 ± 2.5	13.8 ± 2.0	12.4 ± 2.3	13.6 ± 1.5
	Ac-PSMA + 1 μM	111.2 ± 29.6	18.8 ± 7.8	12.8 ± 0.4	12.4 ± 3.2	11.7 ± 4.7
PC-3	Ac-PSMA alone	100.0 ± 0.0	83.2 ± 13.4	86.4 ± 11.1	81.5 ± 13.0	63.5 ± 13.2
	Ac-PSMA + 0.1 μM	107.2 ± 4.5	49.3 ± 24.3	49.4 ± 26.9	48.3 ± 23.9	41.1 ± 22.9
	Ac-PSMA + 1 μM	99.6 ± 5.0	47.0 ± 23.5	48.5 ± 27.0	47.5 ± 24.4	34.6 ± 3.9
	Activity [^{177}Lu] [kBq]	***0***	***78***	***313***	***1250***	***5000***
C4-2	Lu-PSMA alone	100.0 ± 0.0	95.4 ± 6.6	91.6 ± 4.9	81.4 ± 6.1	53.8 ± 5.2
	Lu-PSMA + 0.1 μM	118.7 ± 22.3	65.3 ± 12.7	68.2 ± 3.4	66.6 ± 5.6	52.0 ± 11.9
	Lu-PSMA + 1 μM	111.2 ± 29.6	67.6 ± 0.3	61.4 ± 2.1	53.8 ± 0.6	39.6 ± 2.7
PC-3	Lu-PSMA alone	100.0 ± 0.0	95.7 ± 2.5	100.4 ± 10.0	95.8 ± 12.8	93.4 ± 21.7
	Lu-PSMA + 0.1 μM	107.2 ± 4.5	89.5 ± 7.5	87.1 ± 2.3	88.4 ± 5.6	81.4 ± 0.7
	Lu-PSMA + 1 μM	99.6 ± 5.0	78.8 ± 1.4	81.5 ± 1.2	82.0 ± 4.9	81.4 ± 1.7

Data are presented as fluorescence signal normalized to untreated control and expressed as percent of control (mean ± standard deviation) for TRT alone and in combination with two concentrations of the DNA-PK inhibitor Nedisertib® across the administered activity range. Cell viability was assessed using a resazurin-based fluorescence assay. Values represent a minimum of three independent experimental repetitions.

somatostatin-receptor models.[15] They further highlight that different assays capture distinct aspects of TRT biology, such as initial DNA damage versus long-term proliferative capacity, underscoring the need to consider endpoint-specific sensitivity when interpreting TRT effects.

Furthermore, a key addition to our work compared with earlier studies is the systematic comparison of PSMA-bound and nontargeted radionuclides, providing new insight into how targeting-associated properties, particularly activity localization, influence TRT efficacy. In the cell lines PSMA-bound activity is partially internalized, whereas nontargeted activity predominantly remains at the cell membrane. Both assays, γH2AX and cell viability, demonstrated that the internalization of the short-range α-emitter is essential for efficacy but has minimal impact for the longer-range β^--emitter, reflecting pronounced differences in linear energy transfer (high vs low) and particle range (50-100 μm vs 1-2 mm) that translate into distinct patterns of DNA damage induction and cellular viability. Likewise, prior work with the β^--emitter ^{161}Tb has shown that membrane versus cytoplasmic distribution does not meaningfully alter biological outcomes, a finding mirrored in our study by the nonsignificant differences between PSMA-bound and nontargeted ^{177}Lu.[19] Our results have direct implications for the rational design of future radiopharmaceuticals and underscore distinct requirements for α- and β^--emitters. While α-emitters require rapid internalization and intracellular retention to achieve maximal biological effect, longer-range β^--emitters with cross-fire capabilities are less dependent on internalization and primarily benefit from sustained and high-density membrane binding. Consequently, α-emitter–based therapies are inherently more reliant on homogeneous target expression and sufficient target accessibility, whereas β^--emitters are more tolerant of heterogeneous target distribution within tumors.

Beyond these findings, the long-term DNA damage analyses provide further insight into the radiobiological distinctions between these emitter types. The larger and brighter γH2AX foci, together with visible α-tracks in the nucleus, provide clear evidence of the formation of complex, clustered DNA lesions characteristic of high linear energy transfer (LET) radiation that are inherently difficult to repair. The persistent γH2AX signal up to 72 hours after ^{225}Ac exposure shows that these lesions remain unresolved for extended periods. In contrast, the smaller, less intense foci observed after ^{177}Lu and external photon irradiation are consistent with predominantly simple DSBs that are more readily repaired. This similarity between β^--particles and photons reflects their shared low LET characteristics and suggests they may operate through comparable radiobiological mechanisms, in contrast to high LET α-particles.

These mechanistic differences were mirrored in the long-term cell viability results, which showed markedly greater cytotoxicity with ^{225}Ac than with ^{177}Lu, far exceeding the difference suggested by initial γH2AX levels. The sustained accumulation of irreparable DNA damage after α-TRT exposure likely drives these enhanced antiviability effects. Moreover, the ability of ^{225}Ac to reduce cell viability even in the PSMA-negative, least radiosensitive PC-3 line reinforces the capacity of α-TRT to overcome radioresistance. However, interpreting long-term treatment effects would benefit from complementary clonogenic survival analyses, considered the

gold standard for assessing radiation-induced reproductive cell death, which may provide additional insight into the contribution of reproductive cell death and cell line-specific radiosensitivity.

In the clinical setting, emerging resistance to both β^-- and α-based TRT underscores the need for combination strategies that intensify DNA damage and circumvent repair-driven treatment escape. As Kratochwil et al[4] showed, such resistance can be associated with alterations in DNA-repair pathways, including mutations in key DNA repair genes. In parallel, dose-limiting toxicities associated with high administered activities, including xerostomia, create a compelling rationale for approaches that maintain or enhance efficacy while reducing the overall activity burden. In this context, inhibition of DNA-PK, a central component of the major nonhomologous end-joining repair pathway, represents a promising yet still underexplored strategy for TRT combination. Although preclinical data remain limited, 2 studies to date have evaluated TRT in combination with DNA-PK inhibitors: one used BAY-8400 together with ^{227}Th in LNCaP cells, and another examined AZD7648 combined with ^{177}Lu in neuroendocrine tumor models.[20,21] In our study, we selected the commercially available DNA-PK inhibitor Nedisertib, which has previously demonstrated radiosensitizing properties in vivo when combined with external photon irradiation.[22] In contrast to earlier studies that examined individual radionuclides, our work is the first to investigate combination therapy with a DNA-PK inhibitor across all 3 radiation modalities, α- and β^--TRT, as well as external photon irradiation, in multiple PCa cell lines. The results demonstrate a pronounced radiosensitization effect across all radiation modalities, with the strongest enhancement observed for α-TRT. The combination of DNA-PK inhibition with TRT enabled comparable reductions in cell viability at markedly lower activity levels, indicating the potential for substantial activity de-escalation without compromising efficacy. This is particularly relevant for ^{225}Ac, where supply constraints and toxicity concerns at higher administered activities remain major barriers to broader clinical implementation. While ^{177}Lu does not exhibit the same magnitude of activity de-escalation potential with combination therapy, its radiosensitization effect through DNA-PK inhibition may still offer meaningful benefit in selected clinical contexts, especially when therapy resistance limits monotherapy effectiveness. Overall, these findings underscore that DNA-PK inhibition, most notably when paired with α-TRT, can broaden the therapeutic window and support clinically relevant reductions in administered activity.

Conclusions

In summary, this work provides a comprehensive radiobiological comparison of ^{225}Ac and ^{177}Lu within a uniform experimental framework and provides insights into mechanistic principles that may inform TRT optimization for metastatic castration-resistant PCa. By integrating activity-resolved γH2AX analyses, long-term cell viability assays, and activity localization-dependent effects, we demonstrate that the superior radiobiological effectiveness of α-emitters is driven by persistent complex DNA damage distinct from the more repairable lesions induced by β^--emitters or external photon irradiation. Our data establish the activity ranges required for comparable effects with ^{177}Lu and highlight the assay-dependent nature of α:β^- potency ratios, underscoring the need to validate results with complementary biological endpoints. They further emphasize the importance of standardized experimental conditions, including uniform treatment times, defined activity ranges, and optimized assay formats, to enable meaningful cross-study comparisons in the TRT field.

In addition, this study provides considerations that may inform the rational design and optimization of radiopharmaceuticals. As demonstrated, α-emitter efficacy depends strongly on internalization and homogeneous target expression, whereas β^--emitters benefit primarily from high membrane-binding affinity and may remain effective even with heterogeneous target expression.

Finally, DNA-PK inhibition with Nedisertib enhanced TRT response across conditions and was associated with substantial activity de-escalation in our experimental setting, with the greatest benefit observed with α-TRT. Together, these findings provide a mechanistic basis for further investigation of TRT optimization strategies and support future evaluation of combination approaches in more advanced preclinical models and in vivo studies, with the long-term goal of improving TRT efficacy, reducing toxicity, and expanding treatment options for advanced PCa.

Importantly, although focused on PSMA-targeted TRT in PCa, these principles are broadly applicable. By directly linking emitter types, activity- and localization-dependent DNA damage profiles, long-term viability outcomes, and the pharmacological inhibition of DNA repair, this work identifies factors associated with TRT response that may guide future radiopharmaceutical development and optimization studies across additional molecular targets and cancer types. As such, the present work contributes to ongoing efforts toward a more standardized framework for developing and evaluating TRT monotherapy and combination strategies, which may facilitate the systematic investigation of additional radiosensitizing agents and DNA damage response targets beyond DNA-PK inhibition.

Declaration of Generative AI and AI-Assisted Technologies in the Writing Process

During the preparation of this work the authors used Microsoft 365 Copilot in order to assist with language refinement and phrasing. After using this tool/service, the authors reviewed and edited the content as needed and take full responsibility for the content of the publication.

References

1. Primac I, Tabury K, Tasdogan A, Baatout S, Herrmann K. The molecular blueprint of targeted radionuclide therapy. *Nat Rev Clin Oncol* 2025;22:869-894.
2. U.S. Food and Drug Administration. FDA approves Pluvicto for metastatic castration-resistant prostate cancer. Accessed September 9, 2026. https://www.fda.gov/drugs/resources-information-approved-drugs/oncology-cancerhematologic-malignancies-approval-notifications.
3. Karmann A, Rose S, Herrmann K, et al. α-Therapy and combination strategies to overcome resistance and enhance clinical outcomes in prostate cancer. *J Nucl Med* 2025;66:1859-1862.
4. Kratochwil C, Giesel FL, Heussel CP, et al. Patients resistant against PSMA-targeting α-radiation therapy often harbor mutations in DNA damage-repair-associated genes. *J Nucl Med* 2020;61:683-688.
5. Rami A, Rashid NS, Zhong C, et al. Association between DNA damage repair alterations and outcomes to ^{177}Lu-PSMA-617 in advanced prostate cancer. *ESMO Open* 2025;10:104131.
6. Khanna R, Gape PMD, Grayson KC, Patel M, Terry SYA. The power of precision: Unravelling the radiobiology of targeted radionuclide therapy. *Clin Oncol (R Coll Radiol)* 2025;48:103923.
7. Dadgar H, Pashazadeh A, Norouzbeigi N, et al. Targeted radioligand therapy: Physics and biology, internal dosimetry and other practical aspects during 177Lu/225Ac treatment in neuroendocrine tumors and metastatic prostate cancer. *Theranostics* 2025;15:4368-4397.
8. Stokke C, Kvassheim M, Blakkisrud J. Radionuclides for targeted therapy: Physical properties. *Molecules* 2022;27:5429.
9. Karimi H, Shaffer TH, Stauff E, et al. Alpha and beta emitters in translational nuclear medicine: Clinical advances, challenges, and future direction. *Int J Mol Sci* 2026;27:2290.
10. Zitzmann-Kolbe S, Remde Y, Moen I, et al. Biodistribution of free francium-221 and bismuth-213 in tumour-bearing SCID mice after successful development of actinium-225/francium-221 radionuclide generator set-up. *Eur J Nucl Med Mol Imaging* 2025;53:633-646.
11. Benešová M, Schäfer M, Bauder-Wüst U, et al. Preclinical evaluation of a tailor-made DOTA-conjugated PSMA inhibitor with optimized linker moiety for imaging and endoradiotherapy of prostate cancer. *J Nucl Med* 2015;56:914-920.
12. Benešová M, Bauder-Wüst U, Schäfer M, et al. Linker modification strategies to control the prostate-specific membrane antigen (PSMA)-targeting and pharmacokinetic properties of DOTA-conjugated PSMA inhibitors. *J Med Chem* 2016;59:1761-1775.
13. Bauder-Wüst U, Schäfer M, Winter R, et al. Synthesis of tritium-labeled Lu-PSMA-617: Alternative tool for biological evaluation of radiometal-based pharmaceuticals. *Appl Radiat Isot* 2023;197:110819.
14. Lawal IO, Morgenstern A, Vorster M, et al. Hematologic toxicity profile and efficacy of [225Ac]Ac-PSMA-617 α-radioligand therapy of patients with extensive skeletal metastases of castration-resistant prostate cancer. *Eur J Nucl Med Mol Imaging* 2022;49:3581-3592.
15. Graf F, Fahrer J, Maus S, et al. DNA double strand breaks as predictor of efficacy of the alpha-particle emitter Ac-225 and the electron emitter Lu-177 for somatostatin receptor targeted radiotherapy. *PLoS One* 2014;9:e88239.
16. Savio E, Reyes L, Giglio J, et al. Preclinical evaluation of [225Ac]Ac-PSMA-617 and in vivo effect comparison in combination with [177Lu]Lu-PSMA-617 for prostate cancer. *Nucl Med Biol* 2025;146-147:109032.
17. Roobol SJ, van den Bent I, van Cappellen WA, et al. Comparison of high- and low-LET radiation-induced DNA double-strand break processing in living cells. *Int J Mol Sci* 2020;21:6602.
18. Cruz-Nova P, Trujillo-Nolasco M, Aranda-Lara L, Ferro-Flores G, Ocampo-García B. Radiobiological effect of alpha particles. The scientific basis of targeted alpha-particle therapy. *Nucl Med Biol* 2025;146-147:109044.
19. Borgna F, Haller S, Rodriguez JMM, et al. Combination of terbium-161 with somatostatin receptor antagonists-a potential paradigm shift for the treatment of neuroendocrine neoplasms. *Eur J Nucl Med Mol Imaging* 2022;49:1113-1126.
20. Berger M, Wortmann L, Buchgraber P, et al. BAY-8400: A novel potent and selective DNA-PK inhibitor which shows synergistic efficacy in combination with targeted alpha therapies. *J Med Chem* 2021;64:12723-12737.
21. Reuvers TGA, Verkaik NS, Stuurman D, et al. DNA-PKcs inhibitors sensitize neuroendocrine tumor cells to peptide receptor radionuclide therapy in vitro and in vivo. *Theranostics* 2023;13:3117-3130.
22. Damstrup L, Zimmerman A, Sirrenberg C, Zenke F, Vassilev L. M3814, a DNA-dependent protein kinase inhibitor (DNA-PKi), potentiates the effect of ionizing radiation (IR) in xenotransplanted tumors in nude mice. *Int J Radiat Oncol Biol Phys* 2016;94:940-941.